Journal of Marine Research, 46, 883–917, 1988

Plankton dynamics on the outer southeastern U.S. continental shelf. Part II: A time-dependent biological model

by Eileen E. Hofmann[1] and Julie W. Ambler[1]

ABSTRACT

A system of ten coupled ordinary differential equations was developed to investigate the time-dependent behavior of phytoplankton and copepod populations associated with frontal eddy and bottom intrusion upwelling features on the outer southeastern U.S. continental shelf. Model equations describe the interactions of nitrate, ammonium, two phytoplankton size fractions (>10 μm and <10 μm), five copepod categories that represent the developmental stages of a population, and a detrital pool. Formulations for the biological processes are based primarily upon data obtained from laboratory and field experiments for southeastern U.S. continental shelf plankton populations. Time series of nutrient and plankton distributions obtained from GABEX II provide verification of model results.

The simulated time dependent distributions for bottom intrusions show a phytoplankton maximum occurring approximately eight days after the nitrate maximum, and the copepod biomass peaks within eight to nine days after the phytoplankton. Frontal eddy simulations show the same succession except that the short time scale of these events precludes the development of large copepod blooms. To obtain the correct relative abundance of the two phytoplankton size fractions in the bottom intrusion simulations it was necessary to increase the cell death rate of the small (<10 μm) cell size fraction relative to the large cells (.15 d^{-1} vs. .1 d^{-1}). The additional loss from the small cells may represent a transfer to a zooplankton or microzooplankton grazer that is not included in the model. The depth-averaged (20 to 40 m) carbon production calculated from the bottom intrusion simulation was approximately 4 mgC m^{-2} d^{-1} which agrees with production values measured for bottom intrusions.

Model simulations indicate that temperature is a potentially important factor in determining the trophic structure in bottom intrusions. Also the role of frequency of nutrient input, fecal pellet remineralization and phytoplankton growth coefficient in determining the biological distributions in bottom intrusions were evaluated with the model.

1. Introduction

The first study to suggest that plankton productivity of the outer southeastern U.S. continental shelf is affected by periodic inputs of nutrients from upwelled Gulf Stream waters was that of Stefánsson *et al.* (1971). However, their analysis did not reveal the magnitude or extent to which the Gulf Stream influences this region. It is now well documented that Gulf Stream-induced upwelling provides an almost continuous source

1. Department of Oceanography, Texas A&M University, College Station, Texas, 77843, U.S.A.

of nutrients to the outer southeastern U.S. shelf which results in enhanced plankton production. Nutrients are introduced by cold-core Gulf Stream frontal eddies or subsurface intrusions of Gulf Stream water. Upwelling associated with the frontal eddies occurs over a period of a few days; whereas, bottom intrusions may persist for several weeks. The characteristics of these two types of upwelling are summarized in the preceding paper (Ishizaka and Hofmann, 1988, this volume).

Field observations show differences in the biological responses associated with the two upwelling regimes. The episodic upwelling resulting from the frontal eddies produces productive, but short-lived phytoplankton blooms along the outer U.S. southeastern shelf (Yoder *et al.*, 1983; Yoder, 1985). Further, Yoder *et al.* (1983) estimate that approximately 75% of this is "new" production resulting from upwelled nitrate-nitrogen. The phytoplankton populations of these blooms tend to be dominated by small diatoms such as *Skeletonema costatum.* Although copepod abundances do not appear to be greatly affected by the frontal eddy upwelling, pelagic tunicates, especially doliolids, are found in high concentrations in these upwelling features (Atkinson *et al.*, 1978; Deibel, 1985).

Bottom intrusions have been shown to have a large effect on the biology and chemistry of the southeastern U.S. shelf waters (e.g. Dunstan and Atkinson, 1976; Atkinson *et al.*, 1978; Yoder *et al.*, 1983, 1985; Yoder, 1985). The residence time of these features on the shelf is long enough for light-limited phytoplankton to convert nearly all of the upwelled nitrate into plant biomass (Yoder *et al.*, 1983, 1985), which results in large subsurface phytoplankton blooms with an average production that is five times greater than that of the overlying mixed layer. The phytoplankton associated with the bottom intrusions show a successive development from small to large cells, with the later stages of the phytoplankton bloom dominated by large diatoms such as *Rhizosolenia* spp. (Paffenhöfer *et al.*, 1980, 1984; Yoder *et al.*, 1983, 1985; Paffenhöfer and Lee, 1987). Zooplankton concentrations in bottom intrusions can be quite high, approaching 10,000 ind m^{-3}, with *Temora turbinata, Oncaea* spp., *Penilia avirostris* and chaetognaths being the dominant taxa consistently occurring in high abundances in these features (Paffenhöfer, 1983, 1985; Paffenhöfer *et al.*, 1984).

To investigate the dynamics of the lower trophic levels associated with the frontal eddies and bottom intrusions, we developed a ten-component time-dependent biological model which describes interactions among nitrate, ammonium, two phytoplankton size fractions, five categories representing copepod developmental stages, and a detrital pool. Formulations for the biological processes are based upon laboratory and field data resulting from the GABEX I and II programs, which are described in Ishizaka and Hofmann (1988, this volume). An overview of the outer southeastern U.S. continental shelf program is given by Blanton *et al.* (1984).

The time-dependent biological model has a two-fold purpose. The first is to investigate the biological interactions independent of the effects of the circulation, and the second is to provide information concerning the times scales over which the

biological processes operate. Understanding the biological interactions and the time scales over which they occur is necessary to interpret the results of the coupled physical-biological model presented in the following paper (Hofmann, 1988, this volume).

A description of the model governing equations is given in Section 2 and detailed explanations of the model parameter values are given in Section 3. Implementation of the model is discussed in Section 4. Section 5 presents the results of numerical experiments that are designed to test the effect of frequency of nutrient input, temperature, fecal pellet remineralization, and the choice for the maximum assimilation number for phytoplankton growth on the biological distributions and production. Results from these simulations suggest biological mechanisms which may account for the phytoplankton and zooplankton distributions observed in frontal eddies and bottom intrusions. The adequacy of the time-dependent biological model for describing the biological dynamics of the outer southeastern U.S. shelf is considered in Section 6.

2. Model equations

A schematic of the time-dependent biological model is shown in Figure 1. All model components are expressed in terms of μgN l^{-1}. The primary source of nitrogen for this system is nitrate which is supplied through upwelling processes. Additional nitrogen is made available to the phytoplankton as recycled ammonium.

The phytoplankton component has two parts; cells greater than 10 μm (LP) and those less than 10 μm (SP) in size. Separating the phytoplankton in this manner allows estimation of the relative effects of the two size fractions on nutrient uptake and primary production. Also, these two size fractions are consistent with those used in experiments designed to measure primary productivity of the southeastern U.S. continental shelf phytoplankton. Phytoplankton growth is determined by the combined effects of light and nutrient availability. Transfers from the phytoplankton components occur through zooplankton grazing and cell death.

The zooplankton portion of the model consists of a copepod component that is divided into five size categories—eggs to nauplius two (EGGN2), nauplii three and four (N3N4), nauplius five to copepodite three (N5C3), copepodites four and five (C4C5) and adults—which represent development from egg through eleven juvenile stages into adult. The first category is nonfeeding; the remaining four categories feed differentially on the large and small phytoplankton. Transfers from the copepods occur through excretion, egestion of fecal pellets and predation by higher trophic levels. Excretion and fecal pellet mineralization return nitrogen as ammonium. The fraction of fecal pellets not mineralized represents a nitrogen input to the detrital pool. Predation represents the nitrogen transfer to higher trophic levels. Transfers in the copepod components are temperature dependent. The equations used to model the biological processes within each component are given in the following section. Details of the parameters are explained in Section 3.

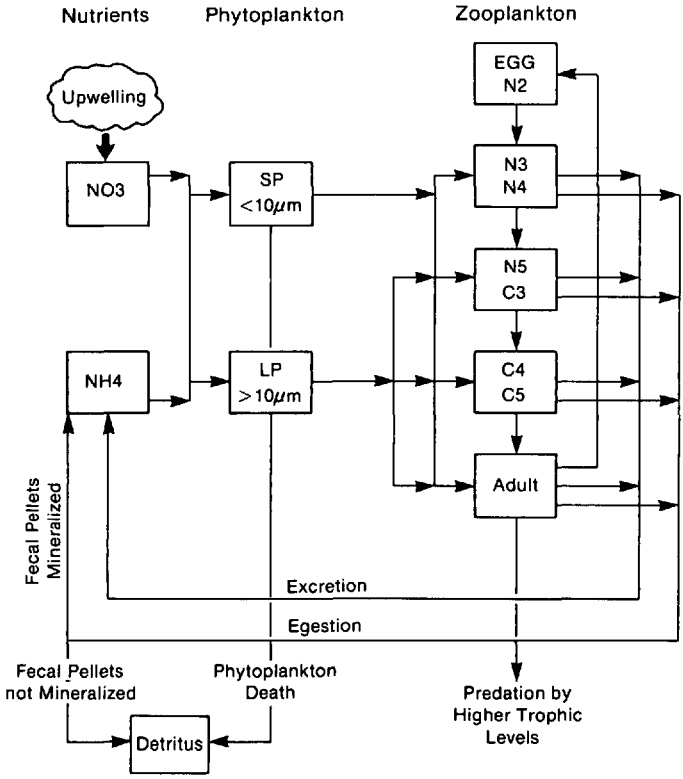

Figure 1. Schematic of the components and biological interactions included in the time-dependent model. See text for explanation.

a. Phytoplankton

Similar dynamics, with different parameter values, were used to model the large and small phytoplankton. The submodel for the two phytoplankton fractions includes terms for phytoplankton growth, cell death, and grazing by the copepod categories. In this model, phytoplankton growth is determined by a multiplicative function that includes the effects of light and ambient nutrients. Mathematical expressions of the large and small phytoplankton dynamics are:

for phytoplankton larger than 10 μm,

$$\frac{dLP}{dt} = \frac{P_m I}{I_k + I}\frac{\mathrm{Chl}}{C}\left[\frac{\mathrm{NO_3}}{k_n + \mathrm{NO_3}}\sigma + \frac{\mathrm{NH_4}}{k_a + \mathrm{NH_4}}\right]LP - \delta LP$$
$$- \sum_{i=3}^{5} \frac{W_{i,1}\,LP}{EPN_i} I_{mi}(1 - e^{-\gamma_i EPN_i})\,ZN_i \qquad (1)$$

for phytoplankton smaller than 10 μm,

$$\frac{dSP}{dt} = \frac{P_m I}{I_k + I}\frac{\mathrm{Chl}}{C}\left[\frac{\mathrm{NO_3}}{k_n + \mathrm{NO_3}}\sigma + \frac{\mathrm{NH_4}}{k_a + \mathrm{NH_4}}\right]SP - \delta SP - \sum_{i=2}^{5}\frac{W_{i,2}SP}{EPN_i} I_{mi}(1 - e^{-\gamma_i EPN_i})ZN_i \tag{2}$$

The first term in Eqs. (1) and (2) represents phytoplankton growth. The second represents cell death and the final term is copepod grazing, where ZN_i is the copepod feeding category. The large phytoplankton are grazed by the three oldest copepod categories. The small cells are grazed by all of the copepod feeding categories. The grazing term is formulated such that the total copepod ingestion is apportioned between the large and small phytoplankton fractions, as described later.

b. Copepods

The copepod component of the time-dependent biological model is based primarily upon laboratory measurements of feeding, egg production and development rates of *Paracalanus* spp. This particular animal, while not always the most abundant species, is found in upwelled waters on the outer southeastern U.S. shelf (Paffenhöfer *et al.*, 1980; Paffenhöfer, 1985). Also, the most complete data set is available for this animal. The copepod submodel includes parameterizations for assimilation, excretion, egg production (adults only), molting and predation processes. These are expressed as follows:

for the nonfeeding category; EGGN2 (ZN_1)

$$\frac{dZN_1}{dt} = \phi E_m(1 - e^{-\lambda(I_5 - E_0)})\,ZN_5 - D_{m_{1,2}}ZN_1 - \left(\frac{M_p ZN_1}{k_1 + ZN_1}\right)ZN_1 \tag{3}$$

for the juvenile categories; N3N4, N5C3 and C4C5 (ZN_2, ZN_3, ZN_4)

$$\begin{aligned}\frac{dZN_i}{dt} = {} & \psi_i I_{mi}(1 - e^{-\gamma_i(EPN_i)})ZN_i - (\eta_i + \upsilon_i EPN_i)ZN_i \\ & + D_{mi-1,i}(1 - e^{-\Lambda_{i-1}EPN_{i-1}})ZN_{i-1} \\ & - D_{mi,i+1}(1 - e^{-\Lambda_i EPN_i})ZN_i - \left(\frac{M_p ZN_i}{k_i + ZN_i}\right)ZN_i\end{aligned} \tag{4}$$

for the adults; ZN_5

$$\begin{aligned}\frac{dZN_5}{dt} = {} & \psi_5 I_{m5}(1 - e^{-\gamma_5 EPN_5})ZN_5 - (\eta_5 + \upsilon_5 EPN_5)ZN_5 \\ & - \phi E_m(1 - e^{-\lambda(I_5 - E_0)})ZN_5 \\ & + D_{m4,5}(1 - e^{-\Lambda_4 EPN_4})ZN_4 - \left(\frac{M_p ZN_5}{k_5 + ZN_5}\right)ZN_5\end{aligned} \tag{5}$$

The terms in Eq. (3) represent egg production by adult copepods, development of the EGGN2 category into the N3N4 category, and predation losses, respectively. The juvenile processes described by Eq. (4) include assimilated ingestion with ψ representing the assimilation efficiency, excretion, development from the preceding category to the present, development from the present category to the next, and predation. For the adults (Eq. 5), the first three terms are assimilation, excretion and egg production, respectively. The molting of the oldest juvenile stage, C4C5, into an adult is given by the fourth term, and the final term represents predation losses. Assimilation, excretion, and molting of the juvenile categories and egg production by the adults are dependent upon the ambient food concentration.

c. Nutrients

The primary nitrogen source for phytoplankton growth in this model is nitrate. The equation governing the time-dependent behavior of this nutrient is of the form,

$$\frac{d\mathrm{NO_3}}{dt} = -\sum_{j=1}^{2}\left[\frac{P_m I}{I_k + I}\frac{\mathrm{Chl}}{C}\frac{\mathrm{NO_3}}{k_n + \mathrm{NO_3}}\sigma\right]P_j + \begin{cases} S_o/L, & \text{for } 0 + n \times (\text{upwelling interval}) < t < L + \\ & n \times (\text{upwelling interval}),\ n = 0, 1, 2, \ldots \\ 0, & \text{for all other times} \end{cases} \tag{6}$$

The first term represents nitrate uptake by the two phytoplankton size fractions, P_j. The second term is a nitrate source which simulates the input of this nutrient by upwelling events. The total nitrate concentration is set by S_o and the time interval over which the nitrate is introduced is determined by L. The time, t, between upwelling events is determined by the upwelling interval.

The time-dependent behavior of ammonium is described as

$$\frac{d\mathrm{NH_4}}{dt} = -\sum_{j=1}^{2}\left[\frac{P_m I}{I_k + I}\frac{\mathrm{Chl}}{C}\frac{\mathrm{NH_4}}{k_a + \mathrm{NH_4}}\right]P_j + \sum_{i=2}^{5}(\eta_i + \upsilon_i EPN_i)ZN_i + \sum_{i=2}^{5}\Gamma_i(1 - \psi_i)I_{mi}(1 - e^{-\gamma_i EPN_i})ZN_i \tag{7}$$

Uptake of ammonium by the two phytoplankton size fractions is given by the first term, and ammonium excretion by the four copepod feeding categories is represented by the second term. The final term is ammonium production through remineralization of the fecal pellets produced by the four copepod feeding categories. The proportion of the fecal pellet production that is remineralized is determined by Γ_i.

d. Detrital pool

For completeness, a detritus equation,

$$\frac{dD}{dt} = \sum_{j=1}^{2}\delta_j P_j + \sum_{i=2}^{5}(1 - \Gamma_i)(1 - \psi_i)(1 - e^{-\gamma_i EPN_i})ZN_i \tag{8}$$

Table 1. Values for phytoplankton parameters. For those parameters that cover a range of values, the value used in the model is given in parenthesis. See text for parameter definitions.

		Value	
Parameter	Units	Frontal eddies	Bottom intrusions
P_m	mgC mgchl $a^{-1}h^{-1}$	15.8	15.5
I_k	eins $m^{-2}h^{-1}$	1.98	1.11
I_o	eins $m^{-2}h^{-1}$	2.2–4.4 (4.0)	1.6–4.6 (4.0)
θ	m^{-1}	0.1	0.09–0.2 (0.1)
chl:c	mgchl:mgC	0.025	0.0104–0.0313 (.025)
V_n	h^{-1}	0.03	0.187
k_n	μM	0.0	1.55
V_a	h^{-1}	0.03	0.176
k_a	μM	0.0	0.047
β	μM^{-1}	5.59	5.59

is also included in the time-dependent biological model. Transfers to this component occur through phytoplankton cell death and the proportion of copepod fecal pellets not remineralized, respectively.

3. Model parameters

a. Phytoplankton growth

The light dependence of phytoplankton growth was modeled with a photosynthesis-light response of the general form

$$P(I) = \frac{P_m I}{I_k + I} \tag{9}$$

where P_m is the maximum assimilation number, I is the light intensity and I_k is the half-saturation light intensity. Yoder *et al.* (1983, 1985) give ranges of values for P_m and I_k that were measured for phytoplankton populations associated with frontal eddies and bottom intrusions and these values are shown in Table 1. The above relationship assumes that the photosynthetic parameters are constant. Eppley (1972), however, suggested that the maximum assimilation number can be predicted from an empirical function that relates carbon assimilation for a twelve-hour day and the temperature dependent specific growth rate as

$$P_m = (2^{\mu} - 1)\frac{C}{\text{Chl}} \tag{10}$$

where $\mu = .085(1.066)^T$ and T is the temperature in degrees Celsius. The effect of a constant versus temperature dependent P_m is evaluated and discussed in the following sections.

Light intensity, I, was modeled as a function of depth and time by

$$I(z, t) = I_o e^{-\theta z} \begin{cases} \sin\left(\frac{t-6}{24}\right)\pi, & \text{for} \quad 6 < t < 18 \\ 0 \quad , & \text{for} \quad t < 6 \text{ or } t > 18 \end{cases} \tag{11}$$

where the maximum photosynthetically active incident radiation at the surface is given by I_o, θ determines the attenuation with depth, z, and t is time in hours. Ranges of values for I_o and θ have been measured for frontal eddies and bottom intrusions in southeastern U.S. shelf waters (Yoder *et al.*, 1983, 1985; Yoder, 1985). These values are shown in Table 1.

The light intensity used in the time-dependent model represents an average value over a depth of 20 to 40 m. This is the approximate depth range covered by a bottom intrusion or frontal eddy. Thus, the model results reflect depth-averaged conditions in these upwelling features. The time dependence of light was modeled with a sine function to give equal periods (twelve hours) of light and dark.

The chlorophyll to carbon ratio in Eqs. 1 and 2 is determined from measurements of changes in particulate matter in frontal eddies (Yoder *et al.*, 1983) and bottom intrusions (Yoder *et al.*, 1985) and values for this ratio are shown in Table 1. For each type of upwelling, ratio values were similar to those obtained for phytoplankton cultures in good physiological condition (Yoder *et al.*, 1985). This is in contrast to the small chlorophyll:carbon ratios measured in the overlying surface mixed layer or in the latter stages of a decaying intrusion that has mixed with surface waters (Yoder *et al.*, 1985).

The uptake of nitrate and ammonium is assumed to follow Michaelis-Menten uptake kinetics of the general form

$$V = \frac{V_m N}{k_s + N} \tag{12}$$

where V_m is the maximum uptake rate of the nutrient, N, and k_s is the nutrient concentration at which $V = V_m/2$. Nitrate uptake as a function of ambient nitrate concentration has been determined for phytoplankton in upwelled waters associated with frontal eddies and bottom intrusions (Fig. 2a). The nitrate uptake rates show a pronounced difference between frontal eddy (spring) and bottom intrusion (summer) upwelling. The spring values are mostly less than .03 hr^{-1} and show little variation with increasing nitrate concentration. Summer values, by contrast, show a response to increasing nitrate concentration that can be described by Eq. (12) and the derived maximum nitrate uptake rate, V_n, and half saturation constant, k_n, are given in Table 1 and Figure 2a. Measurements of ammonium uptake are available only for the summer intrusions (Fig. 2b). This ammonium uptake response can also be described by Eq. (12) (Fig. 2b and Table 1). The half saturation values for nitrate and ammonium uptake in frontal eddies were taken to be zero. This assumes that ammonium uptake in

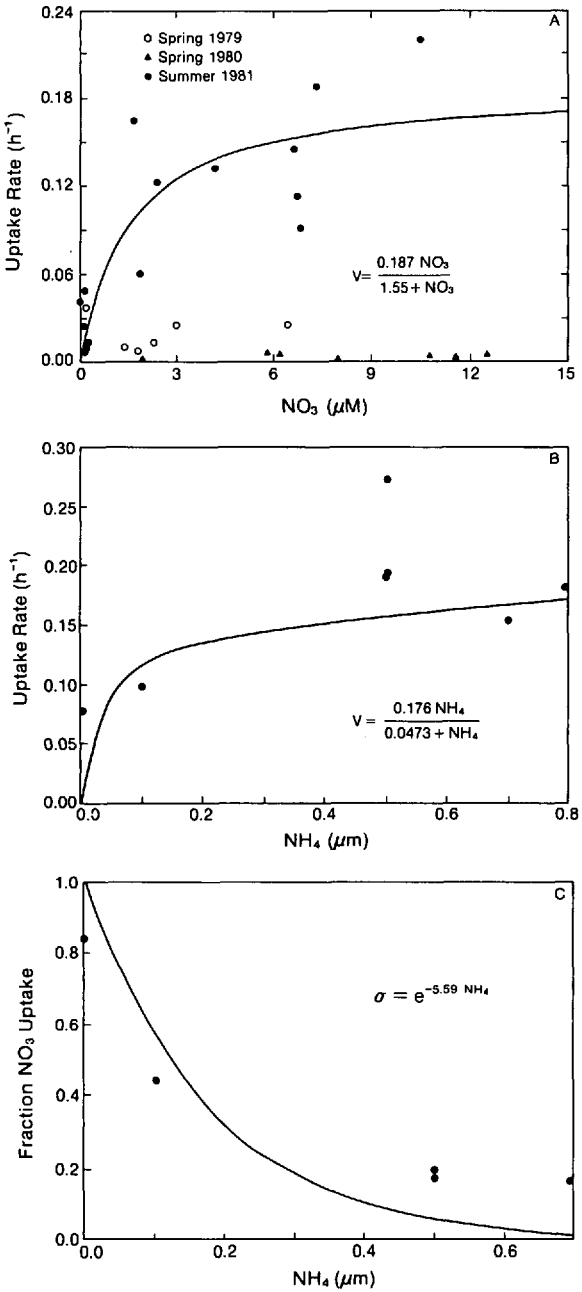

Figure 2. (A) Nitrate uptake rate versus nitrate concentration measured for natural phytoplankton populations associated with frontal eddies (spring) and bottom intrusions (summer). Solid line indicates the curve fit to the summer data and the equation describing the curve is shown. (B) Ammonium uptake rate versus ammonium concentration measured for natural phytoplankton populations associated with bottom intrusions. (C) Nitrate uptake rate as a function of ammonium concentration measured for bottom intrusion waters. The data used to construct the above graphs were provided by Dr. J. A. Yoder.

the frontal eddies is similar to that of nitrate and that both proceed at a constant maximal rate. However, as will be discussed below, the parameterization of phytoplankton growth does not explicitly depend on the value of the maximum nutrient uptake rate.

Numerous studies (see Syrett, 1981 and McCarthy, 1981 for reviews) have shown that nitrate uptake is inhibited by the presence of ammonium. Nutrient preference measurements for phytoplankton occurring in the southeastern U.S. shelf waters during the summer (Fig. 2c) show a decrease of nitrate uptake with increasing ammonium concentration. Using these data, ammonium inhibition of nitrate uptake was modeled as

$$\sigma = e^{-\beta \mathrm{NH}_4} \tag{13}$$

where β determines the decrease of the nitrate uptake with increasing ammonium concentration (Table 1 and Fig. 2c). The above relationship was assumed to apply also to frontal eddy upwelling. The nutrient uptake parameters given in Table 1 were also assumed to apply to both phytoplankton size fractions.

The maximum growth rate for the phytoplankton was taken to be that determined by P_m. This assumes that the maximum growth is set by the ability of the phytoplankton to assimilate carbon. The nitrogen required to support this growth is then subtracted from the available nutrient pool. However, as the ambient nutrients are depleted, phytoplankton growth becomes nutrient limited as well as light limited. Phytoplankton growth as a function of light intensity and ambient nutrient concentration is illustrated in Figure 3a,b. At high nutrient concentrations growth is primarily light limited (Fig. 3a). As the nutrient concentration decreases, growth becomes nutrient limited as well as light limited. As light intensity decreases (Fig. 3b), phytoplankton growth is light limited even at high nutrient concentration. For the depth-averaged (20–40 m) maximum light intensity (~.3 eins m^{-2} h^{-1}), the maximum growth rates (assuming no nutrient limitation) give 2.4 to 3.0 doublings per day for the phytoplankton population.

b. Phytoplankton death

Phytoplankton cell loss is modeled by a linear term where δ represents the fraction of the phytoplankton that is removed each day. This term represents phytoplankton losses in addition to copepod grazing e.g., cell autolysis. Wroblewski (1977) assumed a time scale for cell loss that would reduce a light- or nutrient-limited phytoplankton population to approximately e^{-1} of its initial value in ten days. A similar assumption was made for this model which gives an initial value of δ of .1 d^{-1} for both phytoplankton size fractions. However, as is discussed in Section 4, the final choice for the cell death rates was determined by comparisons of the model distributions to those observed on the southeastern U.S. continental shelf.

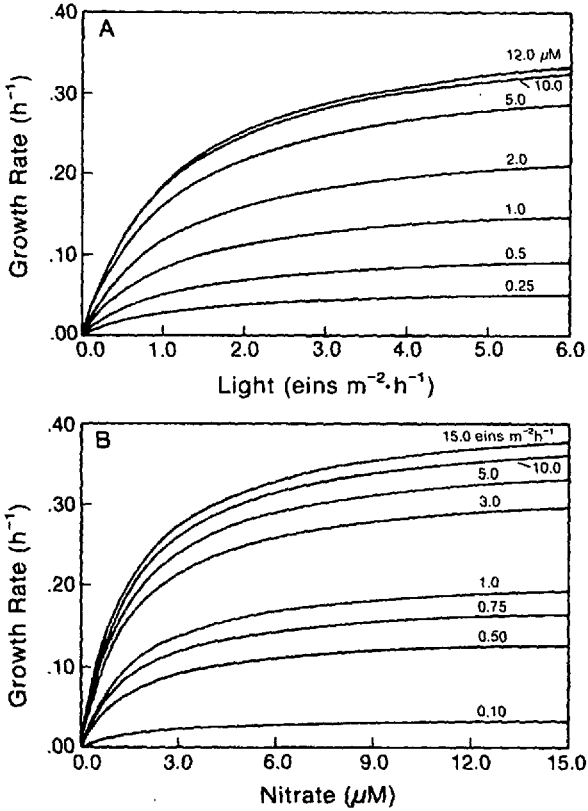

Figure 3. Phytoplankton growth rate at variable nitrate concentrations (A) and variable light intensities (B). See text for explanation.

c. Copepod ingestion and assimilation

The copepod ingestion formulations are based upon data obtained from selective feeding experiments in which *Paracalanus* spp. from the southeastern U.S. shelf waters were fed three concentrations of mixtures of three cultured algae (Paffenhöfer, 1984a). The three algal mixtures were designed to simulate the relative abundance of cells observed in different stages of upwelling. Using these data, Ambler (1986) developed ingestion equations for the *Paracalanus* spp. developmental stages. These equations are a modified Ivlev formulation of the general form,

$$I_i = I_{mi}(1 - e^{-\gamma_i EPN_i}) \qquad \text{for } i = 2, \ldots, 5 \tag{14}$$

where I_{mi} is the maximum ingestion rate, γ_i is a constant affecting the slope of the curve at low food concentration, EPN_i is the effective food concentration (Vanderploeg and Scavia, 1979; Vanderploeg *et al.*, 1984), and i denotes the copepod feeding category. The effective food concentration is a function of copepod body weight and phytoplank-

Table 2. Values for copepod model parameters. See text for parameter definitions.

		Copepod category			
		ZN_2	ZN_3	ZN_4	ZN_5
Parameter	Units				
BW	$\mu g\ N\ an^{-1}$	0.0104	0.0509	0.403	0.880
I_m	d^{-1}	1.096	1.326	1.702	1.872
γ	$1\ \mu g\ N^{-1}$	0.236	0.160	0.096	0.080
W_{j-1}	—	1.0	0.33	0.103	0.085
W_{j-2}	—	0.0	1.0	1.0	1.0
η	d^{-1}	0.3942	0.2613	0.1134	0.1339
ν	$\mu g\ N^{-1}$	0.0062	0.0034	0.0010	0.0005
E_m	d^{-1}	—	—	—	0.5
λ	d^{-1}	—	—	—	1.848
E_o	d^{-1}	—	—	—	0.114
D_m	d^{-1}	0.321	0.193	0.365	—
Λ	$1\ \mu g\ N^{-1}$	1.119	1.102	1.118	—
DR	—	8.32	13.85	7.35	—

ton size fraction (Ambler, 1986). Also, the maximum ingestion rate and γ_i are functions of the copepod body weight (Ambler, 1986). For the model, the median body weight (BW) for each copepod category was calculated from the average of the median weights found at high and low food concentrations in Paffenhöfer's (1984a) selective feeding experiments and these values are given in Table 2. The values for I_{mi} and γ_i were determined for each copepod category (Table 2) from the relationships given in Ambler (1986).

The effective food concentration is also dependent on the phytoplankton concentration, P_j, where j denotes the particular size fraction of cells. This is represented by

$$EPN_i = \sum_{j=1}^{2} W_{i,j} P_j, \text{ for } i = 2, \ldots, 5 \tag{15}$$

where $W_{i,j}$ is a selectivity coefficient which determines the copepod's preference for the particular phytoplankton size fraction, P_j. This formulation assumes that the most preferred phytoplankton size class is filtered 100% efficiently. A detailed discussion of the formulation of the selectivity coefficients for *Paracalanus* spp. is given in Ambler (1986). Values for the selectivity coefficients are given in Table 2 and the dependence of ingestion on effective food concentration for the four feeding categories is shown in Figure 4a–d.

The effective food concentration for the large phytoplankton size fraction was modified to allow for a feeding threshold ($P_j - P_{oi}$). Although Paffenhöfer (1984b) did not observe feeding thresholds for *Paracalanus* spp. experimentally, these were required in the time-dependent model to prevent the three older copepod categories

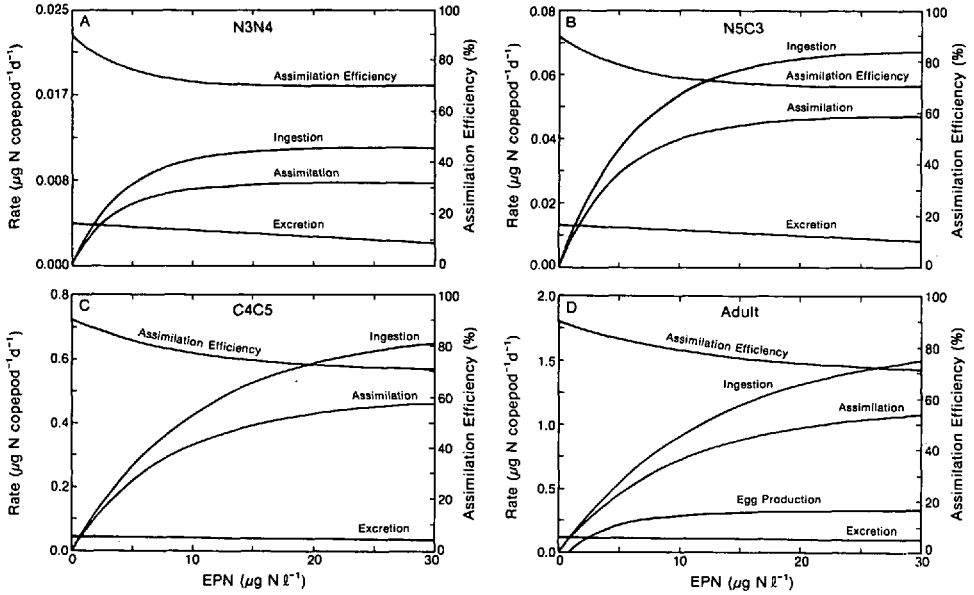

Figure 4. Relationships between the copepod processes and effective food concentration (EPN) for the four feeding categories. See text for explanation.

from grazing the large phytoplankton fraction to extinction. The feeding thresholds were taken to be the nitrogen value equivalent to one copepod per liter (see BW in Table 2). Experimental threshold values (Frost, 1975) were approximately equal to a concentration of one copepod per liter.

Much discussion has surrounded the existence of feeding thresholds (Mullin *et al.*, 1975; Frost, 1975; Kremer and Nixon, 1978; Paffenhöfer, 1984b). In this modeling study the threshold values represent the phytoplankton seed population that is introduced by the advective and diffusive processes associated with a new upwelling event. Assuming a C:N ratio of 6 and Chl:C ratio of .025 the sum of the threshold values are equivalent to a chlorophyll concentration of approximately .2 μg chl a l^{-1} which is within the values reported for southeastern U.S. continental shelf waters prior to an upwelling event (Bishop *et al.*, 1980). Feeding thresholds for the larger phytoplankton size fraction were not necessary in the coupled physical-biological model, supporting the contention that these represent advective and diffusive effects not explicitly included in the biological model. Feeding thresholds were not necessary for the smaller phytoplankton size fraction in either the time-dependent or coupled model.

Feeding by the two youngest copepod feeding categories was assumed to occur continuously over the day-night cycle. The C4C5 and adult categories, however, were assumed to graze at night. The ingestion formulation for these stages was modified

such that grazing increased over a period of two hours from zero to its maximum value, remained at this maximum for eight hours and then decreased linearly to zero. This mimics the diel grazing which can be associated with the older copepod stages (e.g., Mackas and Bohrer, 1976; Dagg and Grill, 1980).

The portion of ingested food that is assimilated by the copepod is determined by the assimilation efficiency. In experimental studies (Kiørboe *et al.*, 1982, 1985; Landry *et al.*, 1984; Murtaugh, 1985) exponential decreases in assimilation efficiency and gut residence time were observed as food concentration increased. Thus, in this model, the assimilation efficiency, ψ, was assumed to be 90% at low food concentrations and to decrease asymptotically to 70% at high food concentrations. Mathematically this is expressed as

$$\psi_i = .3I_i[3 - (.67\, I_i/I_{mi})], \qquad \text{for } i = 2, \ldots, 5 \tag{16}$$

where I_i is the total ingestion and I_{mi} is the maximum ingestion rate for the four copepod feeding categories. This is the assimilation efficiency formulation suggested by Steele and Mullin (1977). Assimilation and assimilation efficiency as a function of food concentration for the four copepod feeding categories are shown in Figures 4a–d. The difference between ingestion and assimilation represents fecal pellet production.

d. Copepod excretion

Excretion (e.g., metabolism in the nitrogen budget) was formulated for the four copepod feeding categories from empirical relationships that relate copepod excretion rate and animal ash-free dry weight (Paffenhöfer and Gardner, 1984). These relationships were obtained from experiments performed with juvenile and adult stages of *Eucalanus pileatus* at two concentrations (1.6 and 48 μg N l^{-1}) of *Thalassiosira weissflogii*. Using the ash-free dry weight values for the *Paracalanus* spp. categories and the excretion rate relationships at the two food concentrations, excretion as a function of food concentration can be expressed as

$$\text{excretion} = \eta_i - \upsilon_i EPN_i \qquad \text{for } i = 2, \ldots, 5 \tag{17}$$

This relationship gives a slight decrease in excretion rate as food concentration increases (Fig. 4a–d). Decreasing excretion rates with increasing food concentration was observed for the *E. pileatus* stages less than 20 μg ash-free dry weight. Since *Paracalanus* spp. is smaller than this size, a decreasing excretion rate is also obtained for all categories of this animal. The excretion rate was assumed to remain constant at food concentrations greater than 48 μgN l^{-1}, which is the highest food concentration used by Paffenhöfer and Gardner (1984).

e. Adult egg production and body weight maintenance

Zooplankton egg production is usually modeled as the difference between assimilation and metabolism (Steele, 1974; Kremer and Nixon, 1978). In this model, the food

assimilated by adult copepods was partitioned into egg production, excretion and body weight maintenance.

Using data obtained from laboratory experiments with *Paracalanus parvus* (Checkley, 1980a), egg production was related to ingestion as

$$EP = \phi E_m(1 - e^{-\lambda(I_5 - E_0)}) \tag{18}$$

where ϕ is the sex ratio (portion of females), E_m the maximum egg production rate, λ is a constant affecting curvature, I_5 is adult ingestion (given by Eq. 14), and E_0 is the ingestion rate below which egg production ceases. Growth experiments (Landry, 1983) suggest that a sex ratio of .83 is reasonable for *Paracalanus* spp. Values for the remaining parameters are given in Table 2 and the relationship of egg production to food concentration is shown in Figure 4d.

Maintenance of the adult body weight is represented by the difference between assimilation and the sum of excretion and egg production (Fig. 4d). The fraction of assimilated nitrogen used to maintain adult body weight has not been measured experimentally. However, when adult females with the same initial body weight are fed different food concentrations, those receiving the highest concentrations produce the most eggs and have the largest body weights within a few days (Durbin *et al.*, 1983).

f. Copepod development rates

Paffenhöfer (unpublished data) found that development of *Paracalanus* spp. from egg to 50% adult at 20°C took 13.9 days at low (5.8 μgN l^{-1}) food concentrations and 12.4 days at high (17.4–30.4 μgN l^{-1}) food concentrations. The percent time spent by *Paracalanus* spp. in each stage was assumed to be the same as that observed for *Paracalanus parvus* (Landry, 1983). With this assumption, maximum developmental rates for the juvenile categories (D_{mi}) were calculated. The developmental rates were related to effective food concentration as

$$D_{i,i+1} = D_{mi}(1 - e^{-\Lambda_i EPN_i}) \tag{19}$$

Values for the maximum development rate, D_{mi} and Λ_i are given in Table 2. Eq. (19) was derived assuming no development without available food.

g. Predation on copepods

Predation on the copepod categories by higher trophic levels was assumed to be of the form

$$P = \frac{M_{pi} Z N_i}{k_i + Z N_i} \qquad \text{for } i = 1, \ldots, 5 \tag{20}$$

where M_{pi} is the maximum predation rate and k_i is the copepod concentration at which

$P = M_{pi}/2$. No data are available for predation rates on zooplankton in southeastern U.S. continental shelf waters and rarely for other systems. Therefore, the maximum predation rates were determined by a series of numerical experiments and are discussed within the context of specific model simulations. The value of k_i was assumed to be .005 μg N l^{-1} for all copepod categories.

h. Copepod temperature dependence

The copepod rate functions for ingestion, egg production, development and predation were formulated for 20°C and then modified to allow for temperature dependence. Temperature dependence for ingestion and predation are available from the literature (Kremer and Nixon, 1978; Huntley and Boyd, 1984) as Q_{10} values. For this modeling study a Q_{10} of 3, which is equivalent to $e^{.110T}$, was assumed for ingestion and predation. The rate equations for these processes were multiplied by the factor, $.111e^{.110T}$, which is 1 at 20°C and increases and decreases in an exponential fashion at temperatures above and below 20°C.

Checkley (1980b) found that copepod egg development could be related to temperature by a Bělehrádek function. A temperature dependent copepod developmental rate was derived using a modified Bělehrádek function of the form

$$D_i(T) = 1/[432DR_i(T + 2.97)^{-2.25}] \qquad \text{for } i = 2, \ldots, 4 \tag{21}$$

where DR_i is the ratio of the minimum development time of a copepod stage to that of egg development at 20°C and T is temperature. The above function replaces D_{mi} in Eq. (19). Values of DR_i for the juvenile copepod categories are given in Table 2; that for the nonfeeding category was 3.64 d^{-1}.

4. Model implementation

a. Initial conditions

Before obtaining solutions to the set of ordinary differential equations described in Section 2, it is necessary to specify initial conditions for the biological variables. The time-dependent biological model is designed to test the effects of frontal eddy and bottom intrusion upwelling on biological populations, therefore, the initial values were set to represent shelf water conditions prior to these upwelling events.

In the absence of upwelling, nitrate concentrations in the outer southeastern U.S. shelf waters are typically less than 0.5 μM (Bishop *et al.*, 1980; Lee and Atkinson, 1983; Atkinson, 1985; Atkinson *et al.*, 1987). When an upwelling event occurs nitrate concentrations can increase to maximum values of 10 to 15 μM with a time scale of two to three days. To simulate the input of nitrate by upwelling events, we used a well established inverse relationship (discussed in Part III) that exists between nitrate and

temperature in newly upwelled waters on the outer southeastern U.S. shelf. The bottom intrusion and frontal eddy upwelling simulations described in the following sections were done using a temperature of 20°C, which corresponds to an initial nitrate concentration of approximately 5 μM. This total nitrate concentration was input over two days.

Ammonium concentrations in southeastern U.S. shelf waters are usually less than 0.1 μM and generally are below the levels of detection for ammonium measurement techniques (Yoder *et al.*, 1983, 1985). Thus, the initial concentration for this nutrient was assumed to be zero.

Initial concentrations for the two phytoplankton size fractions were set at 3 μg N l^{-1}, which corresponds to a chlorophyll concentration of approximately 1.0 μg chl l^{-1} (assuming a nitrogen to chlorophyll ratio of 6). However, as is shown in the following section, the final model solution is independent of the initial phytoplankton concentration.

Initial concentrations for the four youngest copepod categories were assumed to be zero. The adult copepod category concentration was set equal to 0.5 μgN l^{-1} which corresponds to approximately 500 adults m^{-3}. This concentration is at the low end of copepod concentrations observed in southeastern U.S. continental shelf waters (Atkinson *et al.*, 1978; Paffenhöfer *et al.*, 1987). The initial copepod distribution does not affect the final model results. Feeding by the adult copepod category on the phytoplankton bloom produced by the nitrate input initiates the production of copepod eggs. As the model is integrated in time, a copepod cohort develops and comes into adjustment with the other model variables.

b. Verification criteria

The solution method for the system of coupled ordinary differential equations was a fourth order Runge-Kutta with a time step of fifteen minutes. The model was integrated forward in time until repeatable cycles were observed, thereby, eliminating the effects of the initial conditions and transient adjustments on the model solutions. At each time step the total nitrogen (including losses not recycled) in the model was calculated as a check on mass conservation.

Verification of the bottom intrusion and frontal eddy simulation results was accomplished with criteria obtained from field observations of the biological responses to these upwelling events. Nitrate and chlorophyll changes in a bottom intrusion were observed during an event that occurred in the summer 1978 (Yoder *et al.*, 1983). These data show that during the first eight days after the bottom intrusion was stranded on the shelf, nitrate concentrations in the upwelled waters decreased from 7 μM to approximately zero. Chlorophyll concentrations in the intruded waters increased from 1 to >7 μg chl l^{-1}. Of the primary production associated with the bottom intrusion, 50 to 90% was new production resulting from the upwelled nitrate-nitrogen. As chloro-

phyll concentrations increased, the percentage of cells less than 10 μm in size decreased (Yoder *et al.*, 1985). The time difference between chlorophyll and copepod density peaks is more difficult to determine, but for plankton populations associated with bottom intrusions it is in the range of the generation time of the animal: i.e., 10–12 days (Paffenhöfer *et al.*, 1987). Densities as high as 10,000 copepodites and adults per m^3 were observed for the copepod *Temora turbinata*. Assuming equal numbers in each stage this converts to a nitrogen value of approximately 8 μgN l^{-1}.

Observations of the biological responses to frontal eddy upwelling show that these events are characterized by large subsurface phytoplankton blooms. Maximum chlorophyll concentrations in these events approach 6 to 7 μg chl a l^{-1} and occur at depths of 25 to 30 m (Yoder *et al.*, 1983). The phytoplankton blooms associated with the frontal eddies tend to be dominated by diatoms. Copepods do not appear to respond to the frontal eddy upwellings as evidenced by the low zooplankton biomass found in these events (Deibel, 1985).

c. Parameter determination

The ten-component time-dependent biological model described in Section 3 includes in excess of sixty coefficients. Therefore, before running specific numerical experiments, it was first necessary to determine a set of parameters that produces the observed biological interactions in bottom intrusions. The simulation obtained with this model then provides a reference for comparison with those obtained from modified parameter sets.

Many of the coefficients in the time-dependent biological model were specified from data obtained from laboratory and field experiments. However, some parameters are not well defined and, furthermore, the model results are sensitive to the values chosen for these parameters. Ideally, model sensitivity to the less known coefficients should be determined analytically (Tomovic, 1963). However, the large number of coefficients in this model makes this approach unfeasible. Thus, model sensitivity to changes in parameters was determined empirically.

Initial model runs indicated that the phytoplankton death rate and the maximum predation rate on the copepods, which are not defined from observations, had significant effects on the model results. Values for these parameters were determined by comparing the time-dependent behavior of the simulated biological distributions to those observed for plankton populations associated with a bottom intrusion (Yoder *et al.*, 1983). The choice of a particular combination of parameter values was determined by the time interval over which the initial nitrate pulse decreased and by the relative abundance of the two phytoplankton size fractions.

Many numerical experiments with varying cell death rates and maximum predation rates were performed and a subset of these are summarized in Table 3. For each case, the model was run through five cycles, i.e., five upwelling events, which occurred at

Table 3. Summary of model experiments with varying phytoplankton cell death rates and maximum predation rates on the copepods. The number of days required for the disappearance of the upwelled nitrate is shown. Numbers in parenthesis indicate the dominate phytoplankton size fraction. Variable copepod predation rates were .35, .30, .25, .20 and .20 d^{-1} for the youngest to oldest copepod category, respectively.

Cell death rate (d^{-1})		Copepod predation rate (d^{-1})			
LP	*SP*	.1	.2	.3	Variable
.10	.10	7 (<10)	6 (<10)	5 (<10)	6 (<10)
.10	.15	10 (<10)	9 (>10)	8 (>10)	8 (>10)

forty day intervals. The values shown in Table 3 were calculated from the fifth cycle, which eliminates the effects of the transient adjustments that occur during the first two cycles. The forty-day interval between nitrate inputs is chosen primarily for convenience, as this allows sufficient time for the biological interactions to be completed.

Of the cases shown in Table 3, the parameter combination that produced results similar to those observed in bottom intrusion waters is phytoplankton death rates of .1 d^{-1} and .15 d^{-1} for the large and small fractions, respectively and variable predation (highest predation on the youngest categories) on the copepods by the higher trophic levels. These are the values used in the bottom intrusion simulations. However, the variable predation results did not differ greatly from those obtained with a constant maximum predation rate of .3 d^{-1}. In general, increasing the maximum predation on the copepods decreased the time required for the nitrate to be used because less of the phytoplankton biomass was grazed. A higher cell death rate was required for the small phytoplankton size fraction in order to ensure the correct relative abundance of cells. The additional loss from this component (.05 d^{-1}) represents the portion of the $<10\ \mu m$ phytoplankton biomass that could be transferred to other zooplankton grazers such as pelagic tunicates or to microzooplankton.

5. Model results

a. Bottom intrusion simulation

Once the basic parameter set was determined, the time-dependent model was run to investigate biological interactions in bottom intrusions (Fig. 5). After the model has adjusted, the time distribution of the biological variables (Fig. 5a) shows the succession that is expected, with the phytoplankton maximum occurring approximately eight days after the nitrate maximum and the copepod biomass peaking eight to nine days following that of the phytoplankton. Ammonium values are low throughout the simulation with the highest concentrations coinciding with the maximum copepod concentrations.

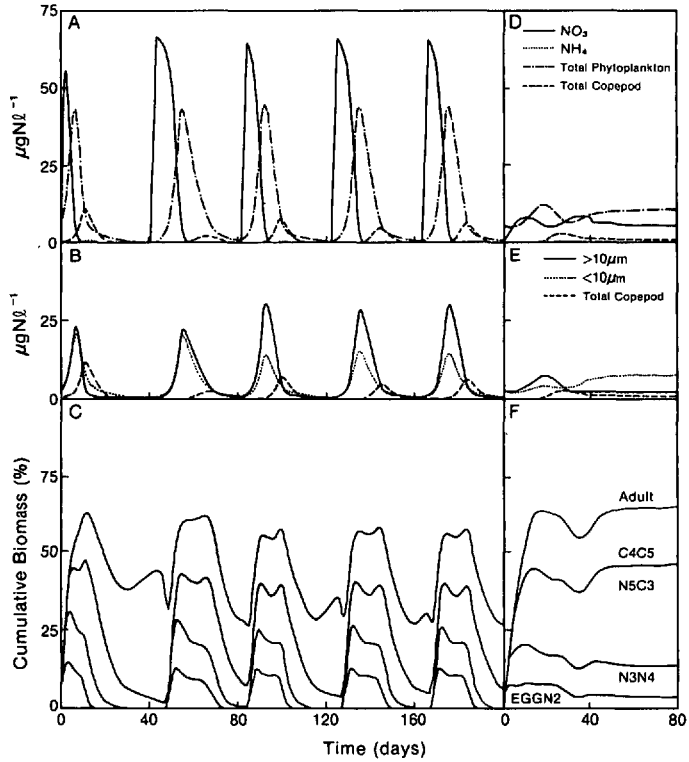

Figure 5. Time-dependent daily-averaged distributions of (A) nitrate, ammonium, total phytoplankton biomass and total copepod biomass and (B) large phytoplankton size fraction (>10 μm), small phytoplankton size fraction (<10 μm), and total copepod biomass. The percent of the total copepod biomass in each category is shown in C. For comparison the time-dependent daily-averaged distributions obtained with a constant nitrate input of 5 μM over forty days are shown in D through F.

The relative abundance of the large and small phytoplankton size fractions over an upwelling cycle is shown in Figure 5b. During the initial stages of the upwelling the concentrations of the two size fractions are approximately equal. However, after approximately ten days, the concentration of the >10 μm size fraction increases and these cells continue as the dominant form until the end of the upwelling cycle. The large cells account for 63% of the total phytoplankton biomass produced during an upwelling cycle.

Each nitrate input initiated a cohort of copepods which produced the age distributions shown in Figure 5c. As can be seen, the adults and juvenile categories (N5 to adults) account for over 60% of the total copepod biomass at the times corresponding to maximum copepod density. The generation time of a cohort can be determined by comparing the times at which the peak biomass occurs for each category. For the

Table 4. Nitrogen and carbon production values for the large and small phytoplankton size fractions calculated from model results. Cumulative values are per forty-day cycle. All values are calculated from the fifth cycle.

	<10 μm	>10 μm	Total
Cumulative new production ($\mu g\ N\ l^{-1}$)	23.7	42.9	66.5
Cumulative regenerated production ($\mu g\ N\ l^{-1}$)	4.5	4.8	9.2
Average nitrogen production ($\mu g\ N\ l^{-1} 40\ d^{-1}$)	30.4	55.1	85.5
Average carbon production ($mgC\ m^{-2}\ d^{-1}$)	1.5	2.4	3.9

Paracalanus spp. in the model, the population generation time is on the order of twelve days and two cohorts are produced during the upwelling cycle.

The portion of new versus regenerated primary production for the two phytoplankton size fractions over an upwelling cycle is shown in Table 4. The percent new production resulting from the upwelled nitrate is 90% and 84% for the large and small size fractions, respectively which is similar to the new production values of 50 to 90% reported by Yoder *et al.* (1985) for bottom intrusion events. The major portion of the primary production occurred within the first six days after the introduction of the nitrate. The primary production resulting from recycled ammonium accounts for only 12% of the total production. The average nitrogen production over the forty-day upwelling cycle represents an average chlorophyll production of 13.7 μg chl a $l^{-1} 40\ d^{-1}$ (assuming C:N of 6). The maximum total phytoplankton concentration in the model is 44 $\mu g\ N\ l^{-1}$ which converts to a chlorophyll concentration of 6.6 μg chl a l^{-1}. This agrees with the maximum chlorophyll values of 7 μg chl l^{-1} observed in bottom intrusions (Yoder *et al.*, 1985).

Integrating the nitrogen production values over the depth of an intrusion (20 m to 40 m) gives an estimate of the total phytoplankton carbon production during the upwelling event. The carbon production associated with the large phytoplankton size fraction is approximately 62% greater than that of the smaller size fraction. The total carbon production value, 3.9 $mgC\ m^{-2}\ d^{-1}$, is at the upper limit of the range of production values (3–4 $mg\ C\ m^{-2} d^{-1}$) measured for bottom intrusions (Yoder *et al.*, 1985).

The cumulative ammonium excretion by the copepod feeding categories over the forty-day upwelling cycle is shown in Table 5. This ammonium plus that produced by fecal pellet remineralization supports the regenerated primary production. From comparing the total regenerated production values in Table 4 to the ammonium excretion values in Table 5, it is obvious that copepod excretion is the primary nitrogen source for the regenerated primary production.

The majority of the total copepod nitrogen production is accounted for by the adult

Table 5. Nitrogen and carbon production values for the five copepod categories calculated from model results. Cumulative values are per forty-day cycle. All values are calculated from the fifth cycle.

	EGGN2	N3N4	N5C3	C4C5	Adult	Total
Cumulative NH_4 excretion ($\mu g\ N\ l^{-1}$)	—	1.8	2.3	1.0	3.4	8.5
Average nitrogen production ($\mu g\ N\ l^{-1} 40\ d^{-1}$)	0.6	0.9	1.9	1.9	5.1	10.4
Average carbon production ($mgC\ m^{-2}\ d^{-1}$)	0.7	0.6	0.7	0.6	0.4	3.0

category (Table 5). The maximum total copepod concentration in the bottom intrusion simulation is 6 $\mu g\ N\ l^{-1}$ which is within the range of concentrations observed for these events (Paffenhöfer *et al.*, 1987).

b. Frontal eddy upwelling

The time-dependent biological model was also used to investigate biological interactions in frontal eddy upwelling events. The primary difference in the parameters for the frontal eddy and bottom intrusion simulations are the values for the half saturation constant for nitrate and ammonium uptake and the photosynthesis versus light response (cf. Table 1). The frontal eddy simulation resulted in time-dependent distributions that do not differ substantially from those obtained for the bottom intrusion and thus are not shown.

The primary difference between the two types of upwelling is the time scale over which the events occur. Frontal eddies exist for only five to seven days; whereas, bottom intrusions can persist for up to six weeks. When the frontal eddy time scale is applied to the biological distributions shown in Figure 5, it is apparent that the biological distributions in the two types of upwelling are different. In the five to seven days following the input of nitrate, the phytoplankton increase in concentration and reach maximum concentration approximately six days after the nitrate maximum. Throughout the first five days of the upwelling, the relative abundance of the two phytoplankton size fractions is approximately the same, but with a slight dominance of the $>10\ \mu m$ fraction. Field observations (Yoder *et al.*, 1983) do not show dominance by any particular size fraction in the frontal eddies.

Copepod concentrations do not begin to increase until about ten days into the upwelling cycle. The implication is that the time scale of the frontal eddies is too short to observe an appreciable response in the copepod populations. This is in fact what is observed in frontal eddies (Deibel, 1985).

Yoder *et al.* (1983) found that the Gulf Stream frontal eddies are characterized by productive, but short-lived phytoplankton blooms. This same behavior occurs in the simulated biological distributions during the first five to seven days after the input of nitrate.

c. Specific numerical experiments

i. Frequency of nutrient input. The bottom intrusion simulation (Fig. 5) shows that approximately twenty days are required to observe the complete cycle from nitrate input to the decay of the copepod bloom. Inputs of nitrate at intervals greater than twenty days do not alter the results shown in Figures 5a–c. The forty-day interval between nitrate pulses was chosen primarily for convenience; however, this choice is not strictly arbitrary. Bottom intrusions occur on the southeastern U.S. shelf with a frequency of four to six weeks. Thus, a forty-day interval between nitrate pulses simulates the frequency at which these events introduce nitrate to shelf waters. However, nitrate inputs at intervals less than those required for nitrate depletion result in the development of biological successions different from those seen in Figures 5a–c. The phytoplankton component does not reach a peak concentration and then decrease, rather it continues to increase because of the increased nitrate concentrations. Rapid inputs of nitrate (intervals less than ten days) might represent the interaction of two intrusions. However, this is not a realistic scenario because field observations do not indicate any mixing between intrusions or one intrusion overriding another. Each event appears to be independent. This time scale of intrusion occurrence is roughly the same as the wind events and Gulf Stream meander cycle (discussed in Ishizaka and Hofmann, 1988, this volume), which are on the order of ten days or more.

For comparison, the results of a simulation with a constant nitrate input over 40 days are shown in Figures 5d–f. This case is analogous to systems in which nitrate is introduced slowly, for example by diffusion across the thermocline in the open ocean. For the constant input simulation the total nitrate introduced over the forty days was equivalent to the two day pulse in the reference simulation. After an initial bloom with a time scale of twenty days, the various model components settle into steady values. In general, the total phytoplankton values are less than in the pulsed simulation and the small cell size fraction dominates. The constant nutrient input results in a higher cumulative copepod biomass which graze preferrentially on the larger cell size fraction. This results in a dominance of the small cell size fraction and concentration of more of the copepod biomass in the younger feeding categories.

ii. Temperature effects. Newly upwelled waters in bottom intrusions range from 18 to 20°C. As these events move on- and alongshore they can be identified as pools of cold subsurface water. Hydrographic data show that in the absence of wind mixing, the temperature of the intruded waters does not increase significantly over the life of the event. If wind mixing occurs while the intrusions are in the shallower inshore waters then warming can occur as the intruded waters are mixed with the surface water. Two simulations were done to test the effect of changing temperature on the biological processes in bottom intrusions. The first represents an intrusion that moves onshore and alongshore without undergoing significant mixing with the surrounding water (Fig. 6a–c). The second simulates an event that moves alongshore for ten days and then

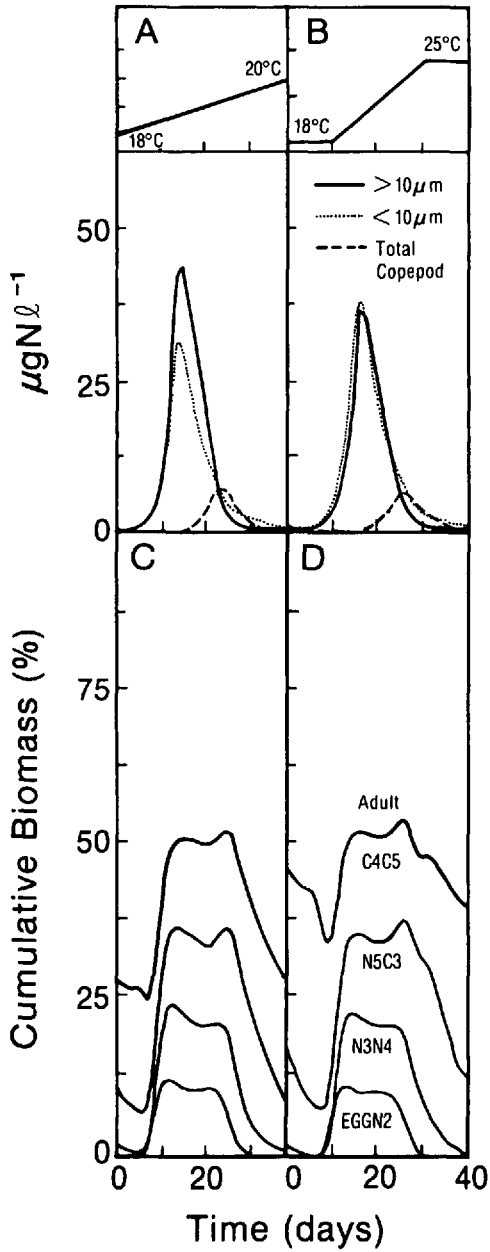

Figure 6. Simulated daily-averaged distributions obtained for time-dependent temperature profiles shown in the top panels. See text for explanation.

moves across the shelf over the next 20 days all the while mixing with the surrounding water (Fig. 6b–d). The maximum temperature in this case is 25°C, which is typical of surface mixed layer water inshore of the 20-m isobath during summer conditions on the southeastern U.S. continental shelf (Atkinson *et al.*, 1987).

The total average phytoplankton nitrogen production over the forty-day cycle for the two temperature scenarios was approximately the same at 150 μgN l^{-1}40 d^{-1}. This represents a 40% increase over the average total nitrogen production obtained with a constant temperature of 20°C. The maximum total chlorophyll concentration for the varying temperature cases was 11.3 μg chl a l^{-1} which is approximately a 40% increase over that calculated for a constant temperature. Chlorophyll concentrations in excess of 10 μg chl a l^{-1} have been observed in bottom intrusion waters (Yoder *et al.*, 1983, 1985). The average total copepod nitrogen production for the two simulations is also approximately equal (13 μg N l^{-1}40 d^{-1}) and represents a 25% increase over that in the constant temperature simulation.

Copepod development and ingestion are each functions of temperature. The decreased temperature initially depresses both processes, thereby allowing the phytoplankton to bloom. As the temperature increases, ingestion by the older feeding categories increases and results in a decrease of the larger size fraction, which is the more preferred food. The higher chlorophyll production results from the decreased grazing pressure during the initial part of the upwelling cycle. Because the large cell size fraction dominates for most of the forty-day period, the age structure of the copepods (Fig. 6c) does not differ significantly from that observed for 20°C.

The primary difference between the simulations shown in Figure 6 is in the relative abundance of the two phytoplankton size fractions and in the age structure of the copepods. For a linear increase in temperature from 18 to 20°C over 40 days, the >10 μm size fraction dominates, but not to the extent observed in 20°C simulation (cf. Fig. 5). The later portion of the upwelling event is dominated by the <10 μm phytoplankton size fraction.

Increasing the temperature from 18 to 25°C over 40 days results in essentially equal abundance of the two phytoplankton size fractions (Fig. 6b). The lower temperatures during the initial portion of the upwelling delays the development of the copepods and hence decreases the grazing pressure on both phytoplankton size fractions. This allows the <10 μm cells to increase. As the temperature increases, copepod ingestion results in preferential removal of the larger cell size fraction. As in the previous case, the diminished copepod ingestion initially results in a more productive phytoplankton bloom during the first part of the upwelling cycle. At temperatures greater than 20°C copepod grazing is enhanced, which results in depletion of the phytoplankton and increased copepod production in the later portion of the upwelling cycle.

The copepod age structure (Fig. 6d) for the 18 to 25°C simulation differs from the previous case primarily by a higher cumulative biomass in the three juvenile categories and decreased biomass in the adult category.

iii. Fecal pellet remineralization. Recycled ammonium may be an important nitrogen source in the late stages of a bottom intrusion. However, data for determining the rate at which ammonium is regenerated by bacterial decomposition of fecal pellets in the southeastern U.S. continental shelf waters are lacking and the importance of this process to the upwelling ecosystems of this region is not well known (Pomeroy *et al.*, 1983; Pomeroy, 1985). Bacterial mineralization (at 18°C) of fecal pellet carbon of *Calanus pacificus* was only about 5% per day (Jacobsen and Azam, 1984) and decomposition rates of sediment trap carbon ranged from 1% to 50% per day (Iseki *et al.*, 1980). Given these rates, it is unlikely that fecal pellet remineralization is a significant nitrogen source for phytoplankton populations associated with the short-lived frontal eddies. However, for the longer lived bottom intrusions this process may be important in the later portion of the upwelling. A modeling study of the vertical fecal pellet flux in southeastern U.S. continental shelf waters (Hofmann *et al.*, 1981) indicated that the smaller copepod stages produce the most fecal pellets, but that these are recycled within the water column and not transported to the bottom. Adult fecal pellet production was less, but accounted for the majority of the vertical flux. Thus ammonium regeneration by fecal pellet remineralization may be significant in the bottom intrusions that are characterized by large copepod blooms.

The effect of fecal pellet remineralization was tested by running the bottom intrusion model with different constant fecal pellet regeneration rates and with regeneration rates that varied with copepod category. The results are summarized in Table 6.

As the fecal pellet regeneration rate increases, the average total phytoplankton nitrogen increases. However, there is only a 6% increase in total average phytoplankton nitrogen from zero to 100% remineralization. While the total phytoplankton nitrogen does not increase greatly, the percent of the total nitrogen that is accounted for by the small (<10 μm) phytoplankton size fraction increases with increasing regeneration rate. During the initial portion of the upwelling both phytoplankton size fractions increase in concentration. The larger fraction is, however, the preferred food source for the three oldest copepod feeding categories. Consequently, these cells are essentially depleted at the end of the forty days. The smaller size fraction is subjected to reduced grazing pressure because of the smaller selectivity coefficients (cf. Table 2) and thus the <10 μm cells are able to use the ammonium as it becomes available. This accounts for the small increase in the <10 μm size fraction at the end of the upwelling cycle (Figs. 5 and 6).

As the fecal pellet remineralization rate increases, the percent regenerated production in each phytoplankton size fraction also increases. In general, the regenerated production associated with the <10 μm size fraction is approximately 6% higher than the larger cell size fraction. Most of this production occurs in the latter half of the upwelling cycle.

There is a small increase in the average total copepod nitrogen between the no

Table 6. Summary of simulation results for varying fecal pellet remineralization rates. Variable rates represent .5, .4, .2 and .1 d^{-1} for the youngest to oldest copepod feeding categories, respectively.

	Proportion fecal pellet remineralization (d^{-1})						
	0.0	0.2	0.4	0.6	0.8	1.0	variable
Average total phytoplankton nitrogen ($\mu g\ N\ l^{-1} 40\ d^{-1}$)	84.4	85.3	86.9	87.8	88.8	89.9	86.3
% <10 μm	34.4	39.4	39.6	41.8	43.9	46.1	39.3
% regenerated production >10 μm	9.3	10.5	11.9	13.2	14.3	15.4	10.7
% regenerated production <10 μm	15.2	17.3	17.9	19.3	20.5	21.6	16.8
% regenerated production supported by fecal pellet remineralization	—	13.7	24.1	31.2	35.8	41.3	17.6
Average total copepod nitrogen ($\mu g\ N\ l^{-1} 40\ d^{-1}$)	10.5	10.9	10.6	10.6	10.6	10.7	10.5
% three youngest copepod feeding categories	44.8	46.7	47.7	47.7	48.7	49.9	46.2

regeneration and 20% d^{-1} regeneration rates which accounts for the decrease in the total phytoplankton nitrogen. However, for the remaining regeneration rates, the total copepod nitrogen decreases slightly. As the percent of small cells increases, the age structure of the copepod categories changes. More of the copepod biomass is accounted for by the three juvenile feeding categories. These stages feed on the smaller cells, with the youngest feeding category feeding exclusively on the <10 μm size fraction. Development from the juvenile through adult categories is dependent upon the effective food concentration. Thus increasing the percent of small cells slows the development of the older juvenile category to adults. The result is that more of the copepod biomass is accounted for by the younger juvenile stages.

iv. Phytoplankton growth coefficient. In the bottom intrusion model the photosynthesis versus light response for the phytoplankton growth was modeled with a Michaelis-Menten curve where P_m and I_k were determined from observations. As a comparison, the model was run with the maximum assimilation number determined from the empirical temperature relationship (Eq. 10) derived by Eppley (1972). The resulting time-dependent distributions are shown in Figure 7.

In general these distributions show broad peaks rather than the sharp rapid changes that are seen in Figure 5. The difference in the phytoplankton distributions obtained with this simulation and those shown in Figure 5 arises because the value of P_m obtained from the temperature relationship (9.3 mg C mg chl $a^{-1}h^{-1}$) is approximately

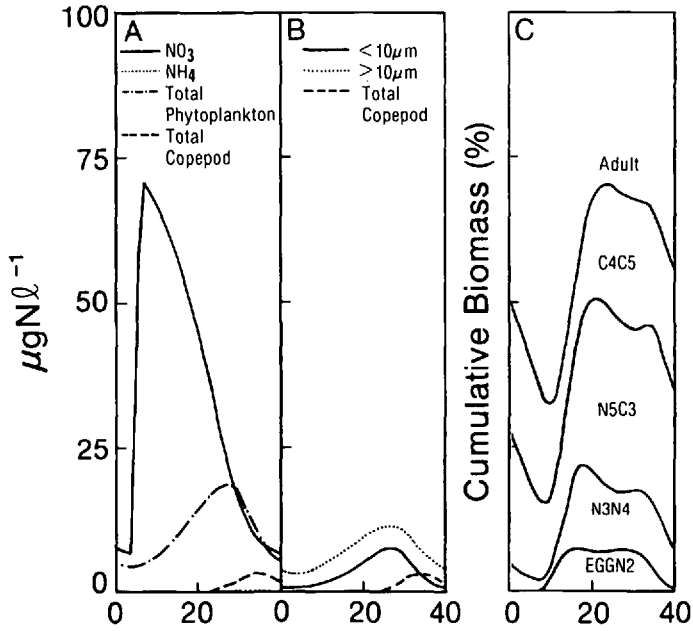

Figure 7. Time-dependent daily-averaged distributions obtained when the maximum assimilation number is determined from temperature. The temperature used in the simulation was 20°C.

half that of the value measured for bottom intrusions and frontal eddies (cf. Table 1). Over the forty-day upwelling cycle, the nitrate is not depleted by the phytoplankton as is observed in bottom intrusion waters. The phytoplankton maximum occurs approximately eighteen days after the nitrate maximum, rather than the six to eight days that is expected. The copepod maximum occurs after approximately thirty days and follows the phytoplankton maximum by eight days. Thus, the time scales that are found in this simulation are considerably longer than those observed in bottom intrusions. Also, the relative abundance of the two phytoplankton size fractions is not correct (Fig. 7b).

The average total phytoplankton nitrogen produced over the forty-day period is 84.2 μgN $l^{-1}40\ d^{-1}$ which is only slightly less than the 85.5 μg N $l^{-1}40\ d^{-1}$ produced in the bottom intrusion simulation. The total phytoplankton carbon production in the two simulations is also similar, 3.8 vs. 3.9 mgC $m^{-2}\ d^{-1}$. However, the primary difference is the time over which this production occurs. In the bottom intrusion case, the majority of the primary production occurs within the first ten days of the upwelling cycle. For the simulation shown in Figure 7, the primary production occurs at a lower level, but takes place over the entire forty-day period. Also, approximately 68% of the total phytoplankton carbon production is accounted for by the >10 μm size fraction.

The average total copepod nitrogen is 7.7 μg N $l^{-1}40\ d^{-1}$ which represents a 27% decrease over that produced in the bottom intrusion simulation. The lower copepod

nitrogen arises because of the dominance of the smaller cells which are not grazed efficiently by the older copepod feeding categories. This is reflected in the age structure of the copepod population (Fig. 7c) with more of the copepod biomass concentrated in the juvenile feeding categories. The longer time scale of the phytoplankton bloom and preferential grazing on the larger cells by the older copepods inhibits the increase of this size fraction.

6. Discussion

The time-dependent biological model presented in the preceding sections represents a classical upwelling food chain in which phytoplankton production is supported primarily by nitrate rather than by ammonium produced by zooplankton excretion or by microbial regeneration of organic matter in the water column or sediments. Evidence for the development of such a food chain in the upwelled waters on the outer southeastern shelf is given by oxygen production versus nitrate consumption data presented by Yoder *et al.* (1985). These data, which are from a bottom intrusion, show that, for at least the first ten days after nitrate is upwelled, oxygen production is inversely related to nitrate uptake by diatoms. The implication is that the phytoplankton are consuming nitrate and producing oxygen, i.e., autotrophic rather than heterotrophic processes dominate. If recycled nitrogen produced by zooplankton excretion were the primary source for the phytoplankton, the oxygen content of the water would not change significantly since zooplankton consumption of oxygen would be balanced by photosynthetic production of oxygen.

Yoder *et al.* (1983, 1985) found that the percent of primary production supported by nitrate in upwelling features on the southeastern U.S. continental shelf was always greater than 50% and could reach 97% during the peak of the phytoplankton bloom in bottom intrusions. However, within waters associated with the late stages of a bottom intrusion, new production supplied less than 10% of the total primary production. For the bottom intrusion simulations, new production accounted for more than 75% of the total primary production for the dominant (>10 μm) phytoplankton size fraction. In the late portion of the upwelling cycle, however, there is a small increase in the <10 μm phytoplankton size fraction that is supported entirely by recycled ammonium.

The short residence time of the frontal eddies would seem to suggest that plankton populations on the southeastern U.S. continental shelf would not derive much benefit from this type of upwelling. However, recent experimental work (Ishizaka *et al.*, 1983) has shown that phytoplankton populations can respond within a few days to newly upwelled nutrients. Field observations show that the frontal eddies are characterized by increased phytoplankton biomass and enhanced primary production (Yoder *et al.*, 1983; Yoder, 1985). Copepod populations, however, do not show an appreciable response to frontal eddy upwelling (Deibel, 1985). The residence time of the bottom intrusions is such that the phytoplankton are able to convert nearly all of the upwelled

nutrients into plant biomass (Yoder *et al.*, 1983, 1985) and large copepod blooms are able to develop (Paffenhöfer *et al.*, 1987).

The values used for the maximum assimilation number (P_m) in the time-dependent biological model are two to three times higher than those reported for other continental shelf ecosystems (Yoder *et al.*, 1985). The implication is that a given amount of phytoplankton biomass yields a relatively high rate of primary production per incident quanta. Thus, the relatively low phytoplankton biomass (chlorophyll a) observed in southeastern U.S. shelf waters gives high rates of primary production (Yoder *et al.*, 1985). Yoder *et al.* (1985) attribute the high primary production of the bottom intrusions to two factors. The first is that the temperature of the intruded waters is always above 15°C which is higher than the water temperature during spring bloom conditions at higher latitudes. The second is that southeastern U.S. shelf waters during summer months are strongly stratified. This results in two phytoplankton populations; those in the surface mixed layer and those below the thermocline in the intruded waters. The phytoplankton in the lower intruded waters are adapted to low mean light intensity and because mixing is reduced these cells are not exposed to high light intensities.

Determining the maximum assimilation number from Eppley's temperature equation results in a value that is approximately half of the value observed for bottom intrusions. The lower value results in time-dependent biological responses that are not in agreement with those observed (cf. Fig. 7). Thus, for the southeastern U.S. shelf phytoplankton populations, temperature alone is not a good indicator of the maximum growth rate. The phytoplankton populations may be well adapted to an environment that is characterized by episodic, subsurface inputs of nutrients. This may explain the rapid increase in biomass and primary production that is observed to occur in the early stages of upwelling in the southeastern U.S. shelf.

Temperature may also be an important factor in determining the zooplankton response to the bottom intrusions as indicated by the simulations shown in Figure 6. Increased grazing at higher temperatures could alter the relative abundance of the phytoplankton size fractions, and hence change the zooplankton species composition in these events.

The time-dependent biological model includes only two size fractions of phytoplankton. The copepod selective feeding behavior is such that the >10 μm size fraction is the most preferred food source. Because of this, it was necessary to increase the death rate of the smaller cells in order to produce the correct relative abundance of the two phytoplankton size fractions. The increased death rate represents a loss from the <10 μm size fraction that is not explicitly included in the model. In a modeling study of the trophic structure of Loch Striven, Steele and Frost (1977) found that the relative size structure of the herbivores and their food was the primary factor governing transfers between the two and the population structure of the phytoplankton and the herbivorous zooplankton. For the southeastern U.S. shelf model, the addition of small

herbivores or microzooplankton that can graze small cells efficiently would result in the correct relative abundance of the phytoplankton size fractions. There are also other potential candidates that could alter the relative abundance of the phytoplankton size fractions in bottom intrusions. Pelagic tunicates, such as *Oikopleura,* spp., *Thalia democratica* and *Dolioletta geyenbauri,* are associated with both bottom intrusions and frontal eddies and sometimes occur in large concentrations (Atkinson *et al.,* 1978; Deibel, 1985; Paffenhöfer, 1985; Paffenhöfer *et al.,* 1987). The inclusion of these organisms, which grow more rapidly than *Paracalanus* spp. and filter a large size range of particles more effectively than the copepods, could account for the additional .05 d^{-1} loss from the small phytoplankton size fraction. Observations from an intrusion in the summer of 1981 show the co-occurrence of doliolids and copepods, but with the doliolid patch offshore of the copepod patch (Paffenhöfer *et al.,* 1987).

The relative abundance of the phytoplankton size fractions may also be modified by including additional phytoplankton components. Laboratory studies (Paffenhöfer and Knowles, 1978; Paffenhöfer, 1984a) have shown that most stages of the small copepods like *Paracalanus* spp. cannot ingest the large *Rhizosolenia* spp. cells that dominate in an old bottom intrusion. The inclusion of a very large cell, >40 μm, ingested by only the oldest copepod feeding categories, would result in a dominance of this size fraction.

Yoder *et al.* (1981) observed small cell *Skeletonema costatum* dominance in frontal eddies and Paffenhöfer and Lee (1987) found that the larger cell diatoms (*Rhizosolenia, Guinardia*) dominated in the later stages of a bottom intrusion. The difference in species composition may be explained on the basis of the residence times of the two upwelling features which could result in physiological differences between the two cell size fractions. As suggested by Turpin and Harrison (1980), frequent nutrient input with rapid dilution, which is analogous to the frontal eddies, would favor the fast-growing small diatoms. The longer residence time of the bottom intrusions results in nutrient-depleted waters and increased copepod biomass. Turpin and Harrison (1979) found that the larger cells with their greater nutrient storage capacity can survive nutrient-depleted periods. Thus, the larger cell diatoms may be able to survive in the nutrient-depleted waters of the old bottom intrusion. Larger cell diatoms have been observed to be actively reproducing in the nutrient-depleted waters of an old intrusion (Paffenhöfer and Lee, 1987). Physiological processes within a cell are not included explicitly in the phytoplankton submodel. Inclusion of cell physiology in models such as this one will have to await the availability of data adequate to model these processes.

The time-dependent biological model does reproduce the major features of the biological processes observed in bottom intrusions and frontal eddies even though the biology included in the model represents only a portion of the food web on the southeastern U.S. continental shelf. Model realism could be improved by including additional components. Potential candidates that could be of importance in the southeastern U.S. continental shelf ecosystems are microzooplankton, as previously

mentioned, and bacteria. The role of microbes in upwelling events in the southeastern U.S. continental shelf is not well understood (Pomeroy, 1985), but could be a potentially important factor in ammonium regeneration in the old intrusions. The time-dependent simulations presented in Moloney *et al.*, (1986) were designed primarily to investigate the effects of microbial regeneration on biological production. These results indicate that microbial remineralization by bacteria and zooflagellates can contribute more to the nitrogen pool than zooplankton remineralization. However, the addition of these processes to the southeastern U.S. continental shelf simulations will have to await the availability of data to adequately describe them.

Validation of a time-dependent biological model, such as the one presented here, should be done using time series measurements of biological distributions. For the outer southeastern U.S. continental shelf, such measurements are not available for frontal eddies and the biological time series data available for bottom intrusions are somewhat sparse. However, the available biological measurements for these two upwelling features do provide comparisons for quantities such as model-derived total primary production and the time scales over which some processes occur. On the basis of these comparisons, the model performs adequately. The real intent of the time-dependent biological model is to present the assumptions and formulations for the biological system and to investigate specific biological scenarios that are of interest for the outer southeastern U.S. continental shelf. The detailed predicted versus observed analysis has been reserved for the coupled physical-biological model presented in the following paper.

Acknowledgments. We thank J. Yoder and G.-A. Paffenhöfer for providing us with the data, some of it unpublished, used to derive the nutrient, phytoplankton and copepod formulations. Their advice and help was invaluable in the development, formulation and implementation of the biological model. Special thanks are extended to G.-A. Paffenhöfer for his comments on an earlier version of this model. His suggestions were most useful in formulating and analyzing the copepod portion of the biological model. Comments by J. Ishizaka were helpful in model development and in analysis of the model results. Thanks are also extended to J. Kremer and one anonymous reviewer for their critical evaluation of this modeling study. Their input resulted in a much improved biological model. This research was supported by the National Science Foundation Grant OCE-8320650.

REFERENCES

Ambler, J. W. 1986. Formulation of an ingestion function for a population of *Paracalanus* feeding on mixtures of phytoplankton. J. Plank. Res., *8*, 957–972.

Atkinson, L. P. 1985. Hydrography and nutrients of the southeastern U.S. continental shelf, *in* Oceanography of the Southeastern U.S. Continental Shelf, L. P. Atkinson, D. W. Menzel and K. A. Bush, eds., 77–92.

Atkinson, L. P., T. N. Lee, J. O. Blanton and G. A. Paffenhöfer. 1987. Summer upwelling on the southeastern continental shelf of the U.S.A. during 1981: Hydrographic observations. Prog. Oceanogr., *19*, 231–266.

Atkinson, L. P., G.-A. Paffenhöfer and W. M. Dunstan. 1978. The chemical and biological effect of a Gulf Stream intrusion off St. Augustine, Florida. Bull. Mar. Sci., *28,* 667–679.

Bishop, S. S., J. A. Yoder and G.-A. Paffenhöfer. 1980. Phytoplankton and nutrient variability along a cross-shelf transect off Savannah, Georgia, U.S.A. Estuar. Coast. Mar. Sci., *11,* 359–368.

Blanton, J. O., L. P. Atkinson, T. N. Lee, C. R. McClain, D. W. Menzel, G.-A. Paffenhöfer, L. J. Pietrafesa, L. R. Pomeroy, H. L. Windom and J. A. Yoder. 1984. A multidisciplinary oceanography program on the southeastern U.S. continental shelf. EOS, *65,* 1202–1203.

Checkley, D. M., Jr. 1980a. The egg production of a marine planktonic copepod in the sea off Southern California. Limnol. Oceanogr., *25,* 430–446.

—— 1980b. Food limitation of egg production by a marine, planktonic copepod in the sea off Southern California. Limnol. Oceanogr., *25,* 991–998.

Dagg, M. J. and D. W. Grill. 1980. Natural feeding rates of *Centropages typicus* females in the New York Bight. Limnol. Oceanogr., *25,* 597–609.

Deibel, D. 1985. Blooms of the pelagic tunicate, *Dolioletta gegenbauri:* Are they associated with Gulf Stream frontal eddies? J. Mar. Res., *43,* 211–236.

Dunstan, W. M. and L. P. Atkinson. 1976. Sources of new nitrogen for the South Atlantic Bight, *in* Estuarine Processes, Vol. 1, M. Wiley, ed., Academic Press, New York, 69–78.

Durbin, E. G., A. G. Durbin, T. J. Smayda and P. G. Verity. 1983. Food limitation of production by adult *Acartia tonsa* in Narragansett Bay, Rhode Island. Limnol. Oceanogr., *28,* 1199–1213.

Eppley, R. W. 1972. Temperature and phytoplankton growth in the sea. Fish. Bull., *70,* 1063–1085.

Frost, B. W. 1975. A threshold feeding behavior in *Calanus pacificus.* Limnol. Oceanogr., *20,* 263–266.

Hofmann, E. E. 1988. Plankton dynamics on the outer southeastern U.S. continental shelf. Part III: A coupled physical-biological model. J. Mar. Res., *46,* (this volume), 919–946.

Hofmann, E. E., J. M. Klinck and G.-A. Paffenhöfer. 1981. Concentrations and vertical fluxes of zooplankton fecal pellets on a continental shelf. Mar. Biol., *61,* 327–335.

Huntley, M. and C. M. Boyd. 1984. Food limited growth of marine zooplankton. Am. Nat., *124,* 455–478.

Iseki, K., F. Whitney and C. S. Wong. 1980. Biochemical changes of sedimented matter in sediment trap in shallow coastal waters. Bull. Plankton Soc. Japan, *27,* 27–36.

Ishizaka, J. and E. E. Hofmann. 1988. Plankton dynamics on the outer southeastern U.S. continental shelf. Part I: Lagrangian particle tracing experiments. J. Mar. Res., *46,* (this volume.), 853–882.

Ishizaka, J., M. Takahashi and S. Ichimura. 1983. Evaluation of coastal upwelling effects on phytoplankton growth by simulated culture experiments. Mar. Biol., *76,* 271–278.

Jacobsen, T. R. and F. Azam. 1984. Role of bacteria in copepod fecal pellet decomposition: colonization, growth rates and mineralization. Bull. Mar. Sci., *35,* 495–502.

Kiørboe, T., F. Møhlenberg, and K. Hamburger. 1985. Bioenergetics of the planktonic copepod *Acartia tonsa:* relation between feeding, egg production and respiration, and composition of specific dynamic action. Mar. Ecol. Prog. Ser., *26,* 85–97.

Kiørboe, T., F. Møhlenberg and H. Nicolajsen. 1982. Ingestion rate and gut clearance in the planktonic copepod *Centropages hamatus* (Lilljeborg) in relation to food concentration and temperature. Ophelia, *21,* 181-194.

Kremer, J. N. and S. W. Nixon. 1978. A Coastal Marine Ecosystem, Springer-Verlag, 217 pp.

Landry, M. R. 1983. The development of marine calanoid copepods with comment on the isochromal rule. Limnol. Oceanogr., *28,* 614–624.

Landry, M. R., R. P. Hassett, V. Fagerness, J. Downs, and C. J. Lorenzen. 1984. Effect of food acclimation on assimilation efficiency of *Calanus pacificus*. Limnol. Oceanogr., *29*, 362–364.

Lee, T. N. and L. P. Atkinson. 1983. Low-frequency current and temperature variability from Gulf Stream frontal eddies and atmospheric forcing along the southeast U.S. outer continental shelf. J. Geophys. Res., *88*, 4541–4567.

Mackas, P. and R. Bohrer. 1976. Fluorescence analysis of zooplankton gut contents and an investigation of diel feeding patterns. J. Exp. Mar. Biol. Ecol., *25*, 77–85.

McCarthy, J. J. 1981. The kinetics of nutrient utilization, *in* Physiological Bases of Phytoplankton Ecology, T. Platt, ed., 211–233.

Moloney, C. L., M. O. Bergh, J. G. Field and R. C. Newell. 1986. The effect of sedimentation and microbial nitrogen regeneration in a plankton community: a simulation investigation. J. Plank. Res., *8*, 427–445.

Mullin, M. M., E. F. Stewart, and F. J. Fuglister. 1975. Ingestion by planktonic grazers as a function of concentration of food. Limnol. Oceanogr., *20*, 259–262.

Murtaugh, P. A. 1985. The influence of food concentration and feeding rate on the gut residence time of *Dephnia*. J. Plankton Res., *7*, 415–420.

Paffenhöfer, G.-A. 1983. Vertical zooplankton distribution on the northeastern Florida shelf and its relation to temperature and food abundance. J. Plankton Res., *5*, 15–33.

—— 1984a. Food ingestion by the marine planktonic copepod *Paracalanus* in relation to abundance and size distribution of food. Mar. Biol., *80*, 323–333.

—— 1984b. Calanoid copepod feeding: grazing on small and large particles, *in* Trophic Interactions within Aquatic Ecosystems, D. G. Meyers and J. R. Strickler, eds., 75–95.

—— 1985. The abundance and distribution of zooplankton on the southeastern shelf of the United States, *in* Oceanography of the Southeastern U.S. Continental Shelf, L. P. Atkinson, D. W. Menzel and K. A. Bush, eds., 104–117.

Paffenhöfer, G.-A., D. Deibel, L. P. Atkinson, and W. M. Dunstan. 1980. The relation of concentration and size distribution of suspended particulate matter to hydrography in Onslow Bay, North Carolina. Deep-Sea Res., *27*(A), 435–447.

Paffenhöfer, G.-A. and W. S. Gardner. 1984. Ammonium release by juveniles and adult females of the subtropical marine copepod *Eucalanus pileatus*. J. Plankton Res., *6*, 505–513.

Paffenhöfer, G.-A. and S. C. Knowles. 1978. Feeding of marine planktonic copepods on mixed phytoplankton. Mar. Biol., *48*, 143–152.

Paffenhöfer, G.-A. and T. N. Lee. 1987. Summer upwelling on the southeastern continental shelf of the U.S.A. during 1981: Distribution and abundance of particulate matter. Prog. Oceanogr., *19*, 373–401.

Paffenhöfer, G.-A., B. K. Sherman and T. N. Lee. 1987. Summer upwelling on the southeastern continental shelf of the U.S.A. during 1981: Abundance, distribution, and patch formation of zooplankton. Prog. Oceanogr., *19*, 403–436.

Paffenhöfer, G.-A., B. T. Wester and W. D. Nicholas. 1984. Zooplankton abundance in relation to state and type of intrusions onto the southeastern United States shelf during summer. J. Mar. Res., *42*, 995–1017.

Pomeroy, L. R. 1985. The microbial food web of the southeastern U.S. continental shelf, *in* Oceanography of the Southeastern U.S. Continental Shelf, L. P. Atkinson, D. W. Menzel, and K. A. Bush, eds., 118–129.

Pomeroy, L. R., L. P. Atkinson, J. O. Blanton, W. B. Campbell, T. R. Jacobsen, K. H. Kerrick and A. M. Wood. 1983. Microbial distribution and abundance in response to physical and biological processes on the continental shelf of southeastern U.S.A. Cont. Shelf Res., *2*, 1–20.

Steele, J. H. 1974. The Structure of Marine Ecosystems, Harvard University Press, 128 pp.
Steele, J. H. and B. W. Frost. 1977. The structure of plankton communities. Phil. Trans. Roy. Soc. Lond. B, *280*, 485–534.
Steele, J. H. and M. M. Mullin. 1977. Zooplankton dynamics, *in* The Sea, Vol VI, E. D. Goldberg, I. N. McCave, J. J. O'Brien and J. H. Steele, eds., 857–890.
Stefánsson, U., L. P. Atkinson and D. F. Bumpus. 1971. Hydrographic properties and circulation of the North Carolina shelf and slope waters. Deep-Sea Res., *118*, 383–420.
Syrett, P. J. 1981. Nitrogen metabolism of microalgae, *in* Physiological Bases of Phytoplankton Ecology, T. Platt, ed., 182–210.
Tomovic, R. 1963. Sensitivity Analysis of Dynamic Systems, McGraw-Hill Book Company, 142 pp.
Turpin, D. H. and P. J. Harrison. 1979. Limiting nutrient patchiness and its role in phytoplankton ecology. J. Exp. Mar. Biol. Ecol., *39*, 151–166.
—— 1980. Cell size manipulation in natural marine, planktonic, diatom communities. Can. J. Fish. Aquat. Sci., *37*, 1193–1195.
Vanderploeg, H. A. and D. Scavia. 1979. Calculation and use of selectivity coefficients of feeding zooplankton grazing. Ecol. Model., *7*, 135–149.
Vanderploeg, H. A., D. Scavia and J. R. Liebig. 1984. Feeding rate of *Diaptomus sicilis* and its relation to selectivity and effective food concentration of algal mixtures in Lake Michigan. J. Plank. Res., *6*, 919–941.
Wroblewski, J. S. 1977. A model of phytoplankton plume formation during variable Oregon upwelling. J. Mar. Res., *35*, 357–393.
Yoder, J. A. 1985. Environmental control of phytoplankton production on the southeastern U.S. continental shelf, *in* Oceanography of the Southeastern U.S. Continental Shelf, L.P. Atkinson, D.W. Menzel, K.A. Bush, eds., 93–103.
Yoder, J. A., L. P. Atkinson, S. S. Bishop, J. O. Blanton, T. N. Lee and L. J. Pietrafesa. 1985. Phytoplankton dynamics within Gulf Stream intrusions on the southeastern United States continental shelf during summer 1981. Cont. Shelf Res., *4*, 611–635.
Yoder, J. A., L. P. Atkinson, S. S. Bishop, E. E. Hofmann and T. N. Lee. 1983. Effect of upwelling on phytoplankton productivity of the outer southeastern United States continental shelf. Cont. Shelf Res., *1*, 385–404.

Received: *2 December, 1986;* revised: *2 September, 1988.*